Received: 3 July 2018 | Revised: 11 February 2019 | Accepted: 22 March 2019

DOI: 10.1111/jfr3.12541

ORIGINAL ARTICLE

CIWEM Chartered Institution of Water and Environmental Management | Journal of Flood Risk Management | WILEY

A digital elevation model based method for a rapid estimation of flood inundation depth

Salvatore Manfreda | **Caterina Samela**

Department of European and Mediterranean Cultures: Architecture, Environment and Cultural Heritage (DiCEM), University of Basilicata, Matera, Italy

Correspondence
Caterina Samela, Department of European and Mediterranean Cultures: Architecture, Environment and Cultural Heritage (DiCEM), University of Basilicata, 75100 Matera, Italy.
Email: caterina.samela@unibas.it

Funding information
Research agreement between the Civil Protection Department of Basilicata, CINID and DICEM., Grant/Award Number: PCBAS2

Abstract

In recent years, the acquisition of data from multiple sources, together with improvements in computational capabilities, has allowed to improve our understanding on natural hazard through new approaches based on machine learning and Big Data analytics. This has given new potential to flood risk mapping, allowing the automatic extraction of flood prone areas using digital elevation model (DEM) based geomorphic approaches. Most of the proposed geomorphic approaches are conceived mainly for the identification of flood extent. In this article, the DEM-based method based on a geomorphic descriptor—the geomorphic flood index (GFI)—has been further exploited to predict inundation depth, which is useful for quantifying flood induced damages. The new procedure is applied on a case study located in southern Italy, obtaining satisfactory performances. In particular, the inundation depths are very similar to the ones obtained by hydraulic simulations, with a root-mean-square error (RMSE) = 0.335 m, in the domain where 2D dynamics prevail. The reduced computational effort and the general availability of the required data make the method suitable for applications over large and data-sparse areas, opening new horizons for flood risk assessment at national/continental/global scale.

KEYWORDS

DEM-based methods, digital elevation models, flooding, geomorphic flood index, inundation depth, linear binary classification

1 | INTRODUCTION

Society's demand for protection from floods is becoming increasingly pressing (Bradshaw, Sodhi, Peh, & Brook, 2007; Kreibich, Müller, Schröter, & Thieken, 2017; Kundzewicz & Takeuchi, 1999). Therefore, it is critical to integrate detailed studies and identify upscaling strategies on flood hazard and risk assessment (Dottori et al., 2016; Gusyev et al., 2016).

Among flooding characteristics, correct identification of the extent of the exposed areas is the main task for proper flood management. At the same time, the expected inundation depth, flow velocity, and sediment load are essential for adequate planning of flood-prone areas and for minimising flood damages. However, adequate representation of flood propagation, even at small scales, has been a major issue for hydrologists and hydraulic engineers worldwide (Teng et al., 2017).

Given the complexity of natural phenomena, even the most detailed hydraulic models adopt simplifications in order to reproduce the inundation process. Therefore, model predictions are affected by structural errors and limited by the lack of data on real-world flooding events (Aronica, Hankin, & Beven, 1998). As a consequence, achieving flood risk assessment at large scales is still a critical challenge.

Several researchers have tackled this problem, trying to derive a flood hazard/risk mapping on a continental or global scale. Such vast domains imply the adoption of simplifying assumptions and the use of less accurate resolutions; for example, Pappenberger, Dutra, Wetterhall, and Cloke (2012) developed a model cascade to produce hazard maps for several return-periods (2–500 years) for 25 × 25 km grid cells; Winsemius, Van Beek, Jongman, Ward, and Bouwman (2013) developed a framework for global flood risk assessment, leading to hazard maps at 30 arcsec resolution (about 1 km at the equator) demonstrated for Bangladesh; Fluet-Chouinard, Lehner, Rebelo, Papa, and Hamilton (2015) applied a downscaling technique to the Global Inundation Extent from Multi-Satellites (GIEMS) dataset to produce a new high-resolution inundation map at a pixel size of 15 arcsec. Another massive study at global scale was carried out by a consortium of the World Resources Institute (WRI), together with Deltares, VU University of Amsterdam, Utrecht University and the Netherlands Environmental Assessment Agency. They developed the Aqueduct Global Flood Analyzer (Ward et al., 2013; Ward et al., 2014; Winsemius et al., 2013), an open-access web-based interactive platform launched in 2015, which assesses and visualises current and future projections of river flood extent and economic impact at global scale at 30 arcsec resolution (http://floods.wri.org/). Furthermore, an ambitious project of the Joint Research Center (JRC) derived flood hazard maps for Europe and the entire world. Their analyses are based on streamflow data from the European and Global Flood Awareness System (EFAS and GloFAS) and computed using two-dimensional hydrodynamic models for different return periods (from 10 to 200 years) at 30 arcsec resolution (about 1 km at the equator; Alfieri et al., 2014; Dottori et al., 2016).

In parallel with the application of hydraulic models at global scale, alternative geomorphic approaches have been developed with aim of raising awareness about flood hazard at large scale. Since basin morphology keeps track of all past flood events that over the centuries modify and shape the Earth's surface (Manfreda, Di Leo, & Sole, 2011), this field has been increasingly recognised as a potential strategy to fill existing gaps in flood mapping, downscale available data and to support hydraulic modelling and remote sensing applications. These geomorphic approaches are often called DEM-based methods, since they are generally applied using digital elevation models (DEMs). The spatial variation of elevation can be seen as gradients of potential energy which becomes the main physical driver of surface runoff, allowing the modelling of water flow for hydrology (Grabs, Seibert, Bishop, & Laudon, 2009; Hjerdt, McDonnell, Seibert, & Rodhe, 2004; Nobre et al., 2011; Nobre et al., 2016; Rennó et al., 2008) or mass movements such as avalanches and landslides (Gessler, Chadwick, Chamran, Althouse, & Holmes, 2000; Hasegawa, Dahal, Nishimura, Nonomura, & Yamanaka, 2009; Jenson & Dominque, 1988; Moore, Grayson, & Ladson, 1991).

DEM-based methods allow identification of the areas that are geomorphologically prone to inundation (Manfreda, Nardi, et al., 2014a). Over the last years, their success has been greatly enhanced by the perfect match between geomorphic analysis and pattern recognition/machine learning techniques, which explosion has determined continuous improvements in the underlying algorithms. They offer the following advantages: (a) use of data freely available at global scale; (b) dramatic acceleration of computational time; and (c) capacity of mapping at higher resolutions large geographic areas both in data-poor and data-rich environments. Of course, due to their intrinsic nature, they are also affected by a number of limitations, such as an inability to consider the presence of transversal structures (e.g., bridges and culverts) and other man-made features.

Recent analyses on the dominant topographic control for flood exposure using techniques of pattern classification highlighted the potential of a morphologic descriptor, called geomorphic flood index (GFI; Samela, Troy, & Manfreda, 2017), adopted to develop a linear binary classification procedure able to identify flood susceptible areas. This method proved to be cost effective, reliable, and efficient in several test sites in Europe, the United States, and Africa (Manfreda et al., 2015; Manfreda, Samela, et al., 2014b; Samela et al., 2016; Samela, Manfreda, & Troy, 2017; Samela, Troy, & Manfreda, 2017). To train this classifier, an inundation map derived using hydraulic models (or observed from satellite) for a portion of the basin is required (the minimum is 2% of the river basin area). Recently, the full procedure was implemented in an open source QGIS plugin called the Geomorphic Flood Area (GFA) tool (Samela, Albano, Sole, & Manfreda, 2018), allowing users to easily and automatically compute the GFI and turn it into a linear binary classifier capable of detecting flood-prone areas across an entire river basin.

In addition to flood extent, the inundation depth is a key factor in many riverine settings for estimation of direct flood damage. Other factors should also be mentioned (e.g., flow velocity and sediment load), but they require refined studies not always possible at large scales. Therefore, the traditional approaches for flood damage estimation are based on a relationship between flooding depth and expected monetary damage to a specific property or land use. A wide variety of damage functions have been constructed to estimate direct flood damage referring to buildings (Smith, 1994), infrastructures (Dutta, Herath, & Musiake, 2003; Hammond, Chen, Djordjević, Butler, & Mark, 2015; Kellermann, Schönberger, & Thieken, 2016; Scawthorn et al., 2006),

mortality rate (Jonkman, Bočkarjova, Kok, & Bernardini, 2008; Jonkman & Kelman, 2005; Jonkman, Vrijling, & Vrouwenvelder, 2008), and direct damage to vehicles (USACE, 2009). These functions are usually derived from historical data, but it is also possible to adopt simplified methodologies relating water depth (WD) to parameters that can be obtained in absence of in situ measurements (e.g., Yang, Ray, Brown, Khalil, & Yu, 2015).

The use of depth-damage functions is well-suited to large-scale analysis, because the uncertainty of damage estimates decreases over larger sample areas due to the averaging effect (Pistrika, 2010). Conversely, the smaller the spatial unit (individual structures or small cluster of buildings), the poorer the relationship between flood depth and resulting damage (Merz, Kreibich, Thieken, & Schmidtke, 2004; Pistrika & Jonkman, 2010). Therefore, a simplified relationship based on the sole WD may provide reliable indications on flood risk on a large scale.

Considering the relevance of inundation depth for flood risk assessment, the GFI method has been further exploited to obtain an approximate, but immediate, estimate of the water surface elevation in a river and surrounding areas. In this work, the possibility to use the intrinsic properties of the GFI to derive in a simple and efficient way the patterns of flow depth associated to the geomorphic flooded area without further elaborations has been explored.

We believe our findings may help to define new strategies for flood risk studies over large-scale basins, continental or global domains, providing information that, although approximate, may be of practical utility for preliminary assessment of expected flood damage, flood management and mitigation.

2 | METHODS AND MATERIALS

2.1 | The GFI: Flood extent estimation

This procedure stems from the definition of the GFI (Samela, Troy, & Manfreda, 2017), a geomorphic descriptor formulated as an indicator of flood susceptibility. The GFI is defined as the logarithm of the ratio between river depth h_r and the difference in elevation H between the location under examination and the element of the river network closest to it (see Equation (1)),

$$\mathrm{GFI} = \ln\left(\frac{h_r}{H}\right). \tag{1}$$

The river depth h_r is estimated as a function of the upslope contributing area using a hydraulic scaling relationship proposed by Leopold and Maddock (1953) and more recently investigated by Nardi, Vivoni, and Grimaldi (2006) (see Equation (2)),

$$h_r \approx a A_r^{\,n}, \tag{2}$$

where h_r is the WD (m), A_r (km^2) is the contributing area calculated at a point of the river network, a is a scale factor, and n is a dimensionless exponent.

The hydraulic scaling relationship typically follows a power law and might be difficult to calibrate, since it requires paired values of h_r and A_r from a number of gauging stations. In cases where such calibration is not possible, the exponent n can be assigned equal to 0.354 using an average value extracted from literature (see Samela et al., 2018 for further details), while the parameter a can be assigned equal to one since its does not affect subsequent elaborations.

A procedure for the detection of flood-prone areas has been developed using the GFI as a linear binary classifier. This method couples information extracted from the basin morphology—incorporated in the GFI—with information about flood exposure contained in flood hazard maps obtained from hydraulic models. These maps are usually available for small portions of the basin of interest and associated to specific return periods. They are used to train the algorithm and calibrate the optimal threshold, τ, that makes possible to extend the classification between flood-prone and not flood-prone areas over the entire basin. The optimal τ—for the same return period as the flood hazard map used for calibration—is evaluated by iterating the threshold of the classifier and by looking for the minimising of the sum of the false positive rate R_{FP} (overestimation) and the false negative rate R_{FN} (underestimation) calculated by comparison with the official map, assigning equal weights to both rates.

Results of this linear binary classification are not influenced by the parameter a of the scaling relationship reported in Equation (2). In fact, the h_r can be calculated assuming the parameter a equal to one. This implies that the $\ln(a)$ will be included in the computed GFI and therefore its value will be incorporated in the calibrated threshold. In fact, the GFI can be written as

$$\mathrm{GFI} = \ln\left(\frac{h_r}{H}\right) = \ln\left(\frac{a A_r^{\,n}}{H}\right) = \ln(a) + n\ln(A_r) - \ln(H). \tag{3}$$

2.2 | The GFI: Inundation depth estimation

The GFI method, besides giving indications about flood hazard exposure, offers a potential way to derive an estimate of the maximum inundation depth. This is particularly helpful in large-scale analyses and in data poor environments, where it is desirable to exploit to the maximum the available information.

As mentioned in the previous section, the h_r is generally calculated by "neglecting" a in the scaling relationship. In such a case, the obtained GFI′ may be expressed as

$$\mathrm{GFI}' = \mathrm{GFI} - \ln(a) = \ln\left(\frac{A_r^n}{H}\right) = \ln\left(\frac{h_r}{aH}\right). \quad (4)$$

Given this definition, the linear binary classification is used to estimate the relative GFI′ value that identifies the boundary of decision, where h_r and H are equal. Therefore, the estimated optimal threshold τ can be used to derive the parameter a of the scaling function,

$$a = \frac{1}{\exp(\tau)}. \quad (5)$$

In this way, we can correct the values of river stage depth h_r, as illustrated in Equation (2).

Once the water level in the river network is estimated, the most difficult task is to determine the inundation depth in the adjacent areas. From the previously performed geomorphic analysis we know for each point of the river (for each DEM pixel) all the upslope basin locations connected to it, and the difference in elevation H between them (see Figure 1). At this point, we can use the h_r values to estimate, in a simple and direct way, the WD cell by cell of the flood-prone areas, as in Equation (6),

$$\mathrm{WD} = h_r - H. \quad (6)$$

3 | THE STUDY AREA AND DATASET: THE BRADANO RIVER IN SOUTHERN ITALY

The study was carried out on the Bradano River, one of the major rivers of the Basilicata Region (southern Italy). It has a drainage basin of about 2,765 km^2 with an upper portion characterised by a marked topography and a terminal portion characterised by smooth hills and flat valleys. Annual average precipitation ranges from 300 to 700 mm, concentrated in winter between November and January. The mean altitude is about 385 m with about 70% of the basin ranging between 200 and 600 m, and the average slope is about 12% (Canora, D'Angella, & Aiello, 2015). It has a torrential regime with a mean annual discharge of about 7 m^3/s, with severe floods in autumn and winter and almost no river flow during summer.

The portion of the basin near the outlet to the Ionian Sea is one of the richest of the region, with urbanised areas, agricultural activities (with intensive production of fruit, cereals and vegetables), tourist activities (with associated resorts and bathing facilities), and also conservation areas. The same area is also one of the most critical in terms of flooding for both Basilicata and the contiguous Puglia Region, having been hit by several floods in the last few years.

For the present study, we focused on this critical portion near the outlet, investigating an area of about 80 km^2 (Figure 2). We analysed one of the most recent and severe flood events which occurred on December 2–3, 2013. It was induced by heavy rainfall that reached about 100 mm in 1 day (measured at Matera city gauging station upstream from the study area), producing a peak flow discharge recorded in the early hours of December 2 of about 800 m^3/s (Scarpino et al., 2018).

The impact of such flood was studied by Scarpino et al. (2018) using a two-dimensional (2D) hydraulic model named FLORA-2D (FLOod and Roughness Analysis) recently introduced by Cantisani, Giosa, Mancusi, and Sole (2014). The resulting map was adopted for the subsequent studies and the same high-resolution DEM used by Scarpino et al. (2018) for the hydraulic simulation was adopted for the geomorphic analysis. It is a 10-m resolution DEM obtained by a combination of a LiDAR (Light Detection and Ranging) survey and digital aerial photogrammetry, provided by the Interregional

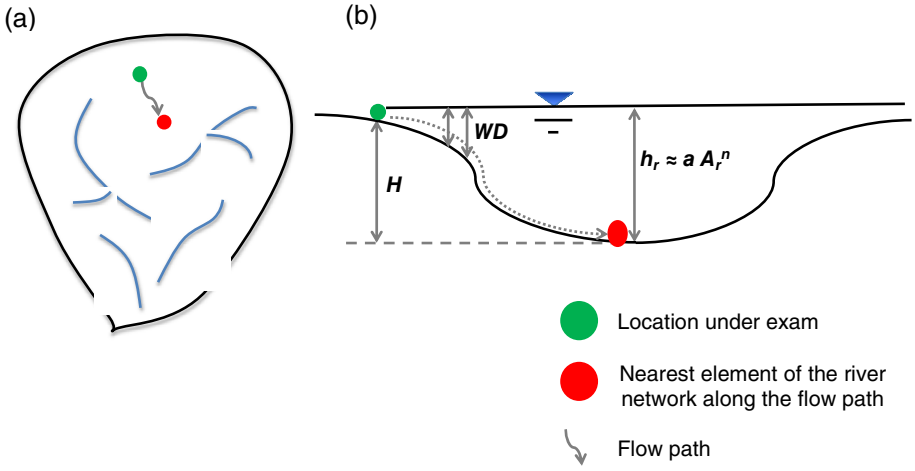

FIGURE 1 A schematic description of the parameters used to derive the geomorphic flood index (GFI) and the water level depth estimated in a hypothetical cross-section

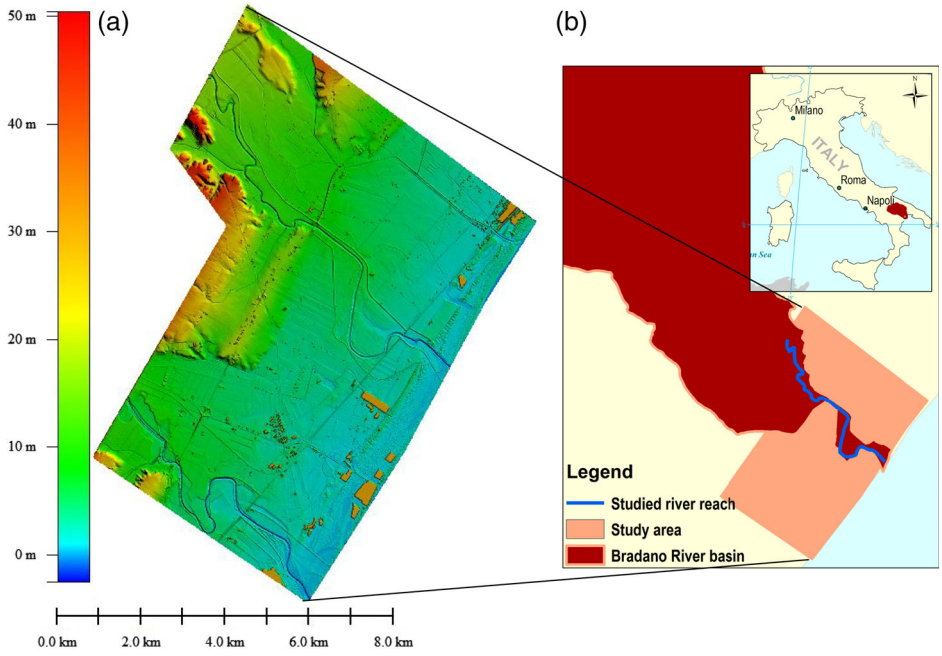

FIGURE 2 LiDAR DEM of the study area with a 10-m resolution (a) and the location of the outlet portion of the Bradano River basin in southern Italy (b)

River Basin Authority of Basilicata. As regards the reference drainage network, it was derived adopting the stream network delineation procedure proposed by Giannoni, Roth, and Rudari (2005).

4 | RESULTS AND DISCUSSION

First, the linear binary classification was carried out using the previously introduced GFA tool. It ran a sequence of computations on the LiDAR DEM to create a hydrologically coherent DEM, define hydrological flow paths, and identify the drainage network. Furthermore, the analyses provided the following essential variables: (a) water level in each cell of the river network, h_r (Figure 3a); (b) difference in elevation of each DEM cell (basin location) to the nearest river H (Figure 3b); (c) derivation of the GFI (Figure 3c); (d) optimal threshold τ; and (e) delineation of the flood-prone areas.

The performances of the GFI as inundation classifier are depicted in Figure 4 using the receiver operating characteristic curve (ROC curve). The ROC curve is created by plotting on the X axis the false positive rate (R_{FP}) against the true positive rate (R_{TP}) plotted on the Y axis at various threshold settings (see Fawcett, 2006). This graphic illustrates the diagnostic ability of a binary classifier as its discrimination threshold is varied. In the present case, it can be noted the strong sensitivity of the GFI in identifying flood-prone areas, as supported by the performances reported in Table 1, which provides the estimated threshold along with the statistics introduced in section 2.1. In particular, it is worth noting the extremely high value of the area under the curve, AUC = 0.94.

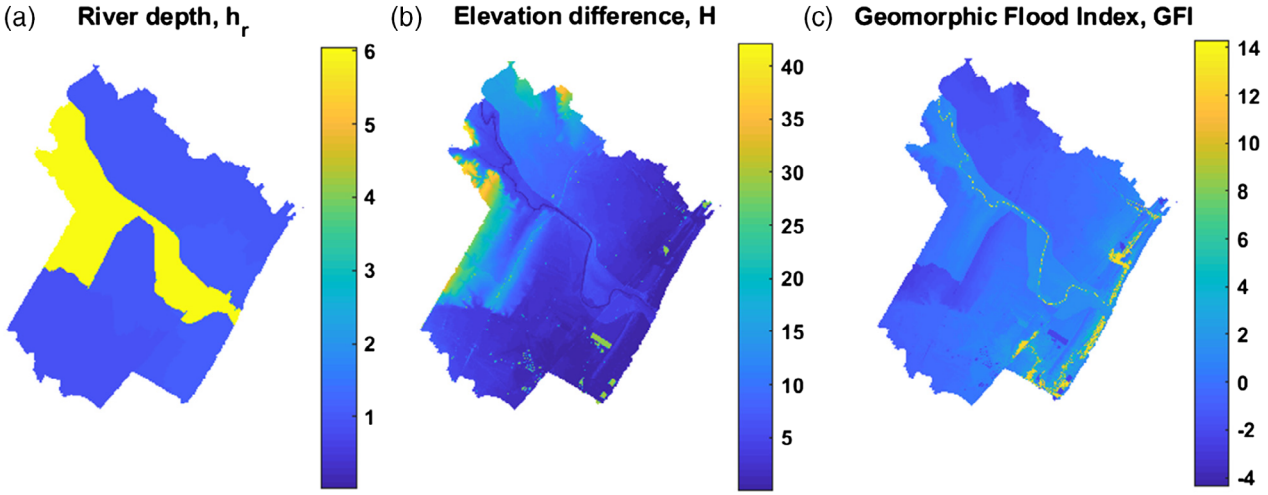

FIGURE 3 Morphological features computed for the outlet of the Bradano basin using the LiDAR DEM with 10 m of resolution

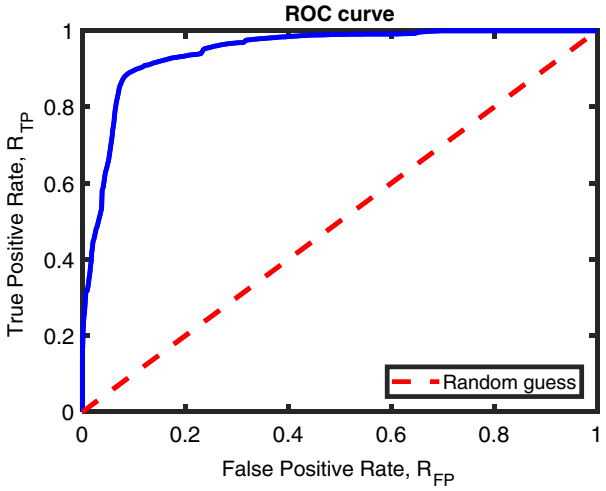

FIGURE 4 Receiver operating characteristics (ROC) curve obtained in calibrating the geomorphic flood index (GFI) at the outlet of the Bradano River basin. The true positive rate and false positive rate have been calculated by comparing the GFI flood-prone areas with the 2D hydraulic model inundation map

In a second step, water level values h_r in each cell of the river network were used to estimate the potential inundation level in all hydrologically linked cells of the study area. This values were used in Equation (6) to determine the geomorphic WD over the DEM domain, which represents a complementary outcome of the geomorphic procedure that has not been calibrated using hydraulic depth simulations. These results can thus be compared and validated with those obtained from the hydraulic simulations, being aware of their limitations. In particular, hydraulic maps obtained from simulations are influenced by the specific considered scenario (e.g., hydrograph adopted, time-step considered, initial conditions used, etc.). In the present case, the reference flood map has been obtained from the envelop of the maximum values observed during a non-stationary event with a peak flow of about 800 m^3/s. Such map represents only one of many possible scenarios since differences may occur due to the interplay between flood hydrograph, water mass transport, overflowing locations, and the inundation dynamics in the adjacent areas (directions and distribution of water in space and time). Instead, the hydrogeomorphic analysis looks at each different cell in a drainage basin individually and establishes how prone to inundation that location is in relation to river morphology.

TABLE 1 Results of the linear binary classification based on the geomorphic flood index (GFI) classifier

Flood extent performances						
τ	R_{TP}	R_{FN}	R_{TN}	R_{FP}	$R_{FP} + R_{FN}$	AUC
−0.423	0.885	0.115	0.902	0.098	0.213	0.941

The comparison between the inundation depths derived by the hydraulic simulation and by the GFI approach are depicted in Figure 5. The two maps have an overall good agreement with some differences that are better addressed in the following. Considering that the hydraulic simulation is strongly influenced by the presence of levees, it seems reasonable to further explore the behaviour of the geomorphic method within the levees and outside this domain where 2D diffusion processes prevail. Thus, two different comparisons were carried out after distinguishing the area along the river within the levees (1D dynamics) and the area outside the levees (2D dynamics). The boundaries of these two domains are identified in Figure 5 with a black solid line.

Since human activities and settlements are usually located outside the floodway, flood risk management is generally more critical in floodplains outside the levees. Therefore, it is particularly instructive to explore the performance of the GFI-derived depth outside the 1D domain.

A comprehensive comparison of the performances of the proposed methodology is given in Figure 6 that provides a scatter plot of the WDs obtained using the geomorphic method (x axis) and the hydraulic model (y axis) in the 1D and 2D domain. The distance from the red line represents the difference in the obtained values. A general overestimation of the inundation depths is noticeable. Both Table 2 and Figure 6 show that while in 1D area the values predicted by the GFI method are rather distant from the hydraulic simulation, outside the levees, where 2D dynamics prevail, the inundation depths are very similar to the ones obtained using the hydraulic model. In both cases, a general overestimation of WD is observed.

A summary of the results is given in Table 2, where the values of the linear correlation coefficient (r) and the root-mean-square error (RMSE) estimated over different domains are reported. These metrics provide an overview of the method performances on different domains. In particular, the correlation between the two patterns is relatively high in all the considered domains, but significant differences are observed in term of RMSE, highlighting a greater reliability of the GFI-derived depths outside the 1D domain.

The differences observed between the two methodologies can be influenced by their structural differences: one considering non-stationarity and the other one neglecting diffusion and transients of flooding process. This leads to differences that become significant especially within the river network.

It should be further stressed that the linear binary classifier has been calibrated using only the extent of the reference inundation map, while the flow depths obtained from the hydraulic modelling have not been used to calibrate the geomorphic WD. For this reason, the two methodologies are forced to reach the same planar extent, but this does not mean that the two datasets are interdependent. In fact, the

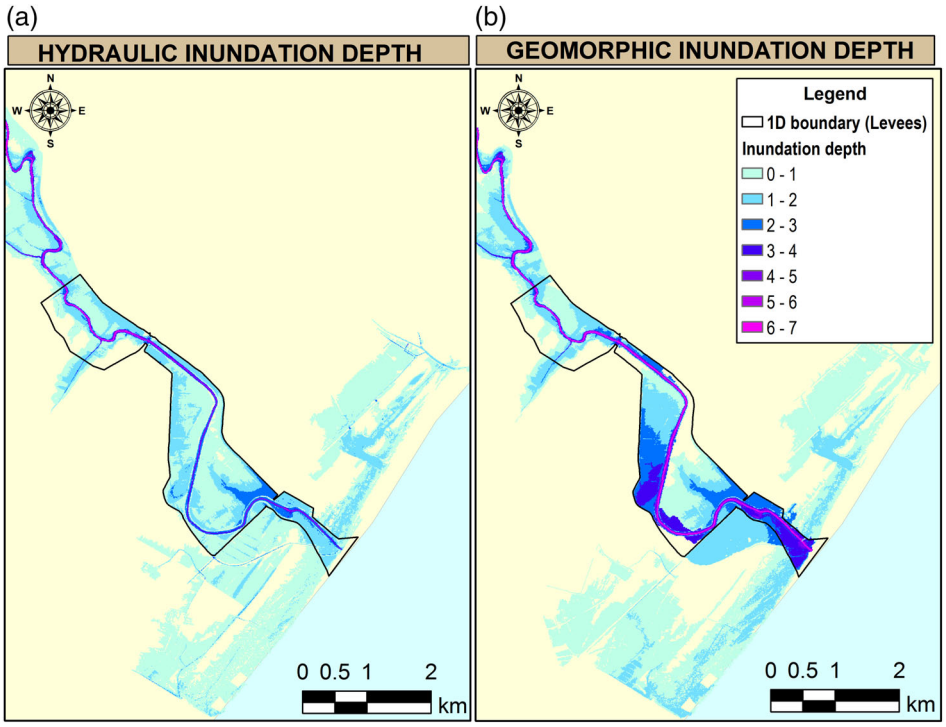

FIGURE 5 The map shows the comparison between the flood hazard maps derived by hydraulic simulations (a) and according to the linear binary classifier based on the geomorphic flood index (GFI) (b). For both panels, the colour gradient represents inundation depths in meters, as reported in the legend

spatial distribution of WD could eventually be optimised to reach the minimum error respect to the reference hydraulic map, but it was our intention to derive the WD using only flood extent. This may represent an advantage for remotely sensed flood mapping that generally provides information only about flood extent. In fact, this kind of information is nowadays available over several areas thank to services like Copernicus Emergency Management Service (Copernicus EMS, https://emergency.copernicus.eu/).

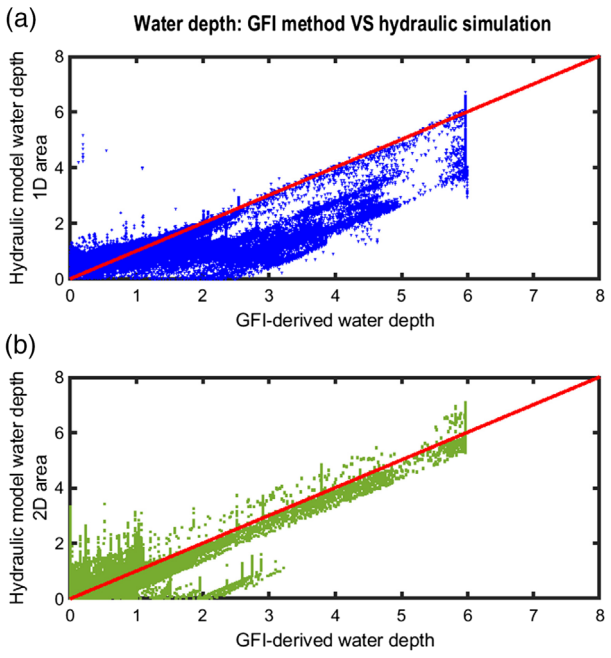

FIGURE 6 Comparison between water depths obtained using the hydrogeomorphic method (x axis) and the hydraulic model (y axis). The comparison was carried out within the 1D domain (a) and 2D domain (b) of the hydraulic simulation, separately. These two domains are separated by the river levees

In this context, it is worthy to mention a recent work by Dottori, Martina, and Figueiredo (2018) that suggested a simplified procedure to derive inundation depth for flood vulnerability assessment. This procedure implies an iterative algorithm of flow diffusion that requires a preliminary description of the hydraulic stage along the river and also a calibration of the friction parameter. This makes the procedure computationally demanding, while the proposed methodology allows a simple and rapid identification of flood depth that can be used for large-scale flood risk assessment studies.

5 | CONCLUSIONS

In data-scarce environments and less developed countries, flood risk is particularly high due to the absence of zoning regulations, flood defence policies and early warning systems, lack of emergency preparedness and, most of all, high population density. In more economically developed countries, even though loss of life is usually lower, property damages and disruptions are still significant despite flood control structures and land use planning. Therefore, there is a critical need to provide tools able to depict the main characteristics of floods in order to support risk assessment.

The proposed approach represents a strategy for flood mapping based only on the use of DEMs that are now freely

TABLE 2 Summary of the performance measures calculated comparing water depths estimated for the mouth of the Bradano River basin using the geomorphic flood index (GFI) method and the FLORA-2D hydraulic model

Inundation depth performances			
	Comparison within the GFI flood-prone areas	**Comparison over the 1D domain of the hydraulic simulation**	**Comparison within the 2D domain of the hydraulic simulation**
Linear correlation coefficient, *r*	.859	.917	.906
Root-mean-square error (m)	0.705	0.620	0.335

available on a global scale. In particular, geomorphic methods are further exploited to provide a description of the inundation WD, which is a critical parameter for flood risk estimation. This result complements the studies on DEM-based methodologies allowing simple, preliminary flood risk mapping on large scales.

This DEM-based methodology can provide a preliminary delineation of flood areas and their potential flood depth with a general tendency to overestimate flood hazard. The flood depth was overestimated in the main stream with a RMSE of 0.62 m, but the approach provides more accurate results in the floodplain with much lower errors (RMSE = 0.335 m). It must be clarified that the geomorphic inundation depth is derived from the parametrisation of the GFA tool calibrated using only the flood extent of a reference flood map.

We are aware that geomorphic procedures cannot describe the flood wave propagation in details and do not replace traditional hydrological–hydraulic studies. Nevertheless, these procedures characterised by simple data requirements can be very useful for administrators, economists, and engineers for management and risk assessment of flood events in case of lack of data.

ACKNOWLEDGEMENTS

This work was carried out within a scientific agreement between the Civil Protection Department of Basilicata, the Interuniversity Consortium for Hydrology (CINID), and the University of Basilicata for the start-up of the Basilicata Hydrologic Risk Centre. The authors would like to thank Dr. Andrea Cantisani (University of Basilicata) for providing the results of the hydraulic studies related to the flood event of December 2013 which was used in the present paper as reference data. We would like to thank reviewers for their insightful comments on the paper, as these comments led us to an improvement of the work.

ORCID

Salvatore Manfreda https://orcid.org/0000-0002-0225-144X
Caterina Samela https://orcid.org/0000-0003-3364-4083

REFERENCES

Alfieri, L., Salamon, P., Bianchi, A., Neal, J., Bates, P., & Feyen, L. (2014). Advances in pan-European flood hazard mapping. *Hydrological Processes*, *28*, 4067–4077. https://doi.org/10.1002/hyp.9947

Aronica, G., Hankin, B., & Beven, K. (1998). Uncertainty and equifinality in calibrating distributed roughness coefficients in a flood propagation model with limited data. *Advances in Water Resources*, *22*, 349–365. https://doi.org/10.1016/S0309-1708(98)00017-7

Bradshaw, C. J. A., Sodhi, N. S., Peh, K. S. H., & Brook, B. W. (2007). Global evidence that deforestation amplifies flood risk and severity in the developing world. *Global Change Biology*, *13*, 2379–2395. https://doi.org/10.1111/j.1365-2486.2007.01446.x

Canora, F., D'Angella, A., & Aiello, A. (2015). Quantitative assessment of the sensitivity to desertification in the Bradano River basin (Basilicata, southern Italy). *Journal of Maps*, *11*, 745–759. https://doi.org/10.1080/17445647.2014.980857

Cantisani, A., Giosa, L., Mancusi, L., & Sole, A. (2014). FLORA-2D: A new model to simulate the inundation in areas covered by flexible and rigid vegetation. *International Journal of Engineering and Innovative Technology*, *3*, 179–186.

Dottori, F., Martina, M. L. V., & Figueiredo, R. (2018). A methodology for flood susceptibility and vulnerability analysis in complex flood scenarios. *Journal of Flood Risk Management*, *11*, S632–S645. https://doi.org/10.1111/jfr3.12234

Dottori, F., Salamon, P., Bianchi, A., Alfieri, L., Hirpa, F. A., & Feyen, L. (2016). Development and evaluation of a framework for global flood hazard mapping. *Advances in Water Resources*, *94*, 87–102. https://doi.org/10.1016/j.advwatres.2016.05.002

Dutta, D., Herath, S., & Musiake, K. (2003). A mathematical model for flood loss estimation. *Journal of Hydrology*, *277*, 24–49. https://doi.org/10.1016/S0022-1694(03)00084-2

Fawcett, T. (2006). An introduction to ROC analysis. *Pattern Recognition Letters*, *27*, 861–874. https://doi.org/10.1016/J.PATREC.2005.10.010

Fluet-Chouinard, E., Lehner, B., Rebelo, L. M., Papa, F., & Hamilton, S. K. (2015). Development of a global inundation map at high spatial resolution from topographic downscaling of coarse-scale remote sensing data. *Remote Sensing of Environment*, *158*, 348–361. https://doi.org/10.1016/j.rse.2014.10.015

Gessler, P. E., Chadwick, O. A., Chamran, F., Althouse, L., & Holmes, K. (2000). Modeling soil–landscape and ecosystem properties using terrain attributes. *Soil Science Society of America Journal*, *64*, 2046. https://doi.org/10.2136/sssaj2000.6462046x

Giannoni, F., Roth, G., & Rudari, R. (2005). A procedure for drainage network identification from geomorphology and its application to the prediction of the hydrologic response. *Advances in Water*

Resources, *28*, 567–581. https://doi.org/10.1016/j.advwatres.2004.11.013

Grabs, T., Seibert, J., Bishop, K., & Laudon, H. (2009). Modeling spatial patterns of saturated areas: A comparison of the topographic wetness index and a dynamic distributed model. *Journal of Hydrology*, *373*, 15–23. https://doi.org/10.1016/j.jhydrol.2009.03.031

Gusyev, M., Gädeke, A., Cullmann, J., Magome, J., Sugiura, A., Sawano, H., & Takeuchi, K. (2016). Connecting global- and local-scale flood risk assessment: A case study of the Rhine River basin flood hazard. *Journal of Flood Risk Management*, *9*, 343–354. https://doi.org/10.1111/jfr3.12243

Hammond, M. J., Chen, A. S., Djordjević, S., Butler, D., & Mark, O. (2015). Urban flood impact assessment: A state-of-the-art review. *Urban Water Journal*, *12*, 14–29. https://doi.org/10.1080/1573062X.2013.857421

Hasegawa, S., Dahal, R. K., Nishimura, T., Nonomura, A., & Yamanaka, M. (2009). DEM-based analysis of earthquake-induced shallow landslide susceptibility. *Geotechnical and Geological Engineering*, *27*, 419–430. https://doi.org/10.1007/s10706-008-9242-z

Hjerdt, K. N., McDonnell, J. J., Seibert, J., & Rodhe, A. (2004). A new topographic index to quantify downslope controls on local drainage. *Water Resources Research*, *40*(5), W05602. https://doi.org/10.1029/2004WR003130

Jenson, S. K., & Dominque, J. O. (1988). Extracting topographic structure from digital elevation data for geographic information system analysis. *Photogrammetric Engineering and Remote Sensing*, *54*, 1593–1600.

Jonkman, S. N., Bočkarjova, M., Kok, M., & Bernardini, P. (2008). Integrated hydrodynamic and economic modelling of flood damage in The Netherlands. *Ecological Economics*, *66*, 77–90. https://doi.org/10.1016/j.ecolecon.2007.12.022

Jonkman, S. N., & Kelman, I. (2005). An analysis of the causes and circumstances of flood disaster deaths. *Disasters*, *29*, 75–97. https://doi.org/10.1111/j.0361-3666.2005.00275.x

Jonkman, S. N., Vrijling, J. K., & Vrouwenvelder, A. C. W. M. (2008). Methods for the estimation of loss of life due to floods: A literature review and a proposal for a new method. *Natural Hazards*, *46*, 353–389. https://doi.org/10.1007/s11069-008-9227-5

Kellermann, P., Schönberger, C., & Thieken, A. H. (2016). Large-scale application of the flood damage model RAilway Infrastructure Loss (RAIL). *Natural Hazards and Earth System Sciences*, *16*, 2357–2371. https://doi.org/10.5194/nhess-16-2357-2016

Kreibich, H., Müller, M., Schröter, K., & Thieken, A. H. (2017). New insights into flood warning reception and emergency response by affected parties. *Natural Hazards and Earth System Sciences*, *17*, 2075–2092. https://doi.org/10.5194/nhess-17-2075-2017

Kundzewicz, Z. W., & Takeuchi, K. (1999). Flood protection and management: Quo vadimus? *Hydrological Sciences Journal*, *44*, 417–432. https://doi.org/10.1080/02626669909492237

Leopold, L. B., & Maddock, T. J. (1953). The hydraulic geometry of stream channels and some physiographic implications. *Geological Survey Professional Paper*, *252*, 57. https://doi.org/10.1016/S0169-555X(96)00028-1

Manfreda, S., Di Leo, M., & Sole, A. (2011). Detection of flood-prone areas using digital elevation models. *Journal of Hydrologic Engineering*, *16*, 781–790. https://doi.org/10.1061/(ASCE)HE.1943-5584.0000367

Manfreda, S., Nardi, F., Samela, C., Grimaldi, S., Taramasso, A. C., Roth, G., & Sole, A. (2014a). Investigation on the use of geomorphic approaches for the delineation of flood prone areas. *Journal of Hydrology*, *517*, 863–876. https://doi.org/10.1016/j.jhydrol.2014.06.009

Manfreda, S., Samela, C., Gioia, A., Consoli, G. G., Iacobellis, V., Giuzio, L., … Sole, A. (2015). Flood-prone areas assessment using linear binary classifiers based on flood maps obtained from 1D and 2D hydraulic models. *Natural Hazards*, *79*, 735–754. https://doi.org/10.1007/s11069-015-1869-5

Manfreda, S., Samela, C., Sole, A., & Fiorentino, M. (2014b). Flood-prone areas assessment using linear binary classifiers based on morphological indices. In *Vulnerability, Uncertainty, and Risk* (pp. 2002–2011). Reston, VA: American Society of Civil Engineers. https://doi.org/10.1061/9780784413609.201

Merz, B., Kreibich, H., Thieken, A., & Schmidtke, R. (2004). Estimation uncertainty of direct monetary flood damage to buildings. *Natural Hazards and Earth System Sciences*, *4*, 153–163. https://doi.org/10.5194/nhess-4-153-2004

Moore, I. D., Grayson, R. B., & Ladson, A. R. (1991). Digital terrain modelling: A review of hydrological, geomorphological, and biological applications. *Hydrological Processes*, *5*, 3–30. https://doi.org/10.1002/hyp.3360050103

Nardi, F., Vivoni, E. R., & Grimaldi, S. (2006). Investigating a floodplain scaling relation using a hydrogeomorphic delineation method. *Water Resources Research*, *42*(9), W09409. https://doi.org/10.1029/2005WR004155

Nobre, A. D., Cuartas, L. A., Hodnett, M., Rennó, C. D., Rodrigues, G., Silveira, A., … Saleska, S. (2011). Height above the nearest drainage—a hydrologically relevant new terrain model. *Journal of Hydrology*, *404*, 13–29. https://doi.org/10.1016/j.jhydrol.2011.03.051

Nobre, A. D., Cuartas, L. A., Momo, M. R., Severo, D. L., Pinheiro, A., & Nobre, C. A. (2016). HAND contour: A new proxy predictor of inundation extent. *Hydrological Processes*, *30*, 320–333. https://doi.org/10.1002/hyp.10581

Pappenberger, F., Dutra, E., Wetterhall, F., & Cloke, H. L. (2012). Deriving global flood hazard maps of fluvial floods through a physical model cascade. *Hydrology and Earth System Sciences*, *16*, 4143–4156. https://doi.org/10.5194/hess-16-4143-2012

Pistrika, A. (2010). Flood damage estimation based on flood simulation scenarios and a GIS platform. *European Water*, *30*, 3–11.

Pistrika, A. K., & Jonkman, S. N. (2010). Damage to residential buildings due to flooding of New Orleans after hurricane Katrina. *Natural Hazards*, *54*, 413–434. https://doi.org/10.1007/s11069-009-9476-y

Rennó, C. D., Nobre, A. D., Cuartas, L. A., Soares, J. V., Hodnett, M. G., Tomasella, J., & Waterloo, M. J. (2008). HAND, a new terrain descriptor using SRTM-DEM: Mapping terra-firme rainforest environments in Amazonia. *Remote Sensing of Environment*, *112*, 3469–3481. https://doi.org/10.1016/j.rse.2008.03.018

Samela, C., Albano, R., Sole, A., & Manfreda, S. (2018). A GIS tool for cost-effective delineation of flood-prone areas. *Computers, Environment and Urban Systems*, *70*, 43–52. https://doi.org/10.1016/j.compenvurbsys.2018.01.013

Samela, C., Manfreda, S., De Paola, F., Giugni, M., Sole, A., & Fiorentino, M. (2016). DEM-based approaches for the delineation of flood-prone areas in an ungauged basin in Africa. *Journal of*

Hydrologic Engineering, *21*, 06015010. https://doi.org/10.1061/(ASCE)HE.1943-5584.0001272

Samela, C., Manfreda, S., & Troy, T. J. (2017). Dataset of 100-year flood susceptibility maps for the continental U.S. derived with a geomorphic method. *Data in Brief*, *12*, 203–207. https://doi.org/10.1016/j.dib.2017.03.044

Samela, C., Troy, T. J., & Manfreda, S. (2017). Geomorphic classifiers for flood-prone areas delineation for data-scarce environments. *Advances in Water Resources*, *102*, 13–28. https://doi.org/10.1016/j.advwatres.2017.01.007

Scarpino, S., Albano, R., Cantisani, A., Mancusi, L., Sole, A., & Milillo, G. (2018). Multitemporal SAR data and 2D hydrodynamic model flood scenario dynamics assessment. *ISPRS International Journal of Geo-Information*, *7*, 105. https://doi.org/10.3390/ijgi7030105

Scawthorn, C., Flores, P., Blais, N., Seligson, H., Tate, E., Chang, S., … Lawrence, M. (2006). HAZUS-MH flood loss estimation methodology. II. Damage and loss assessment. *Natural Hazards Review*, *7*, 72–81. https://doi.org/10.1061/(ASCE)1527-6988(2006)7:2(72)

Smith, D. I. (1994). Flood damage estimation—A review of urban stage-damage curves and loss functions. *Water SA*, *20*, 231–238. https://doi.org/10.1007/978-981-287-365-1_13

Teng, J., Jakeman, A. J., Vaze, J., Croke, B. F. W., Dutta, D., & Kim, S. (2017). Flood inundation modelling: A review of methods, recent advances and uncertainty analysis. *Environmental Modelling and Software*, *90*, 201–216. https://doi.org/10.1016/j.envsoft.2017.01.006

USACE. (2009). *Generic depth-damage relationship for vehicles*. Economic guidance memorandum. Washington, DC: Author.

Ward, P. J., Jongman, B., Kummu, M., Dettinger, M. D., Sperna Weiland, F. C., & Winsemius, H. C. (2014). Strong influence of El Nino Southern Oscillation on flood risk around the world. *Proceedings of the National Academy of Sciences of the United States America*, *111*, 15659–15664. https://doi.org/10.1073/pnas.1409822111

Ward, P. J., Jongman, B., Weiland, F. S., Bouwman, A., Van Beek, R., Bierkens, M. F. P., … Winsemius, H. C. (2013). Assessing flood risk at the global scale: Model setup, results, and sensitivity. *Environmental Research Letters*, *8*, 044019. https://doi.org/10.1088/1748-9326/8/4/044019

Winsemius, H. C., Van Beek, L. P. H., Jongman, B., Ward, P. J., & Bouwman, A. (2013). A framework for global river flood risk assessments. *Hydrology and Earth System Sciences*, *17*, 1871–1892. https://doi.org/10.5194/hess-17-1871-2013

Yang, Y. C. E., Ray, P. A., Brown, C. M., Khalil, A. F., & Yu, W. H. (2015). Estimation of flood damage functions for river basin planning: A case study in Bangladesh. *Natural Hazards*, *75*, 2773–2791. https://doi.org/10.1007/s11069-014-1459-y

How to cite this article: Manfreda S, Samela C. A digital elevation model based method for a rapid estimation of flood inundation depth. *J Flood Risk Management*. 2019;12 (Suppl. 1):e12541. https://doi.org/10.1111/jfr3.12541